Cylindrical Sub-micrometer Confinement Results for the Odd-Symmetric Dimer α,ω-Bis[(4-cyanobiphenyl)-4′-yloxy]undecane (BCB.O11)

M. R. de la Fuente,[†] D. O. López,*[,†,‡] M. A. Pérez-Jubindo,[†] D. A. Dunmur,[†,§] S. Diez-Berart,[‡] and J. Salud[‡]

Departamento de Física Aplicada II, Facultad de Ciencia y Tecnología, Universidad del País Vasco, Apartado 644, E-48080 Bilbao, Spain, Grup de les Propietats Físiques dels Materials (GRPFM), Departament de Física i Enginyeria Nuclear, E.T.S.E.I.B. Universitat Politècnica de Catalunya, Diagonal, 647 08028 Barcelona, Spain, and Departament of Chemistry and Southampton Liquid Crystal Institute, University of Southampton, Southampton, SO17 1BJ, U.K.

Received: December 23, 2009; Revised Manuscript Received: May 5, 2010

Broadband dielectric spectroscopy (10^2 Hz to 1.9×10^9 Hz) and specific heat measurements have been performed on the odd-symmetric dimer α,ω-bis[(4-cyanobiphenyl)-4′-yloxy]undecane (BCB.O11) in the isotropic (I) and nematic (N) phases confined to 200 nm diameter parallel cylindrical pores of Anopore membranes. Unlike previous studies on liquid crystal monomers, untreated and hexadecyltrimethylammonium bromide-treated membranes give rise to radial and axial confinements, respectively. An attempt is made to explain these unexpected results by means of a qualitative model for the dimer arrangement on alumina substrates. The model suggests that the population of conformers, which follow the bulk-like dynamics, is modified by confinement. Such a fact seems to be consistent with other distinctive features attributed to confinement, as for example, the increasing of the entropy change at the N-to-I phase transition for both axial and radial confinements. Specific-heat measurements have shown how confinement affects the N-to-I phase transition by a downward shift in transition temperature as well as by broadened and rounded specific-heat peaks. However, these modifications are revealed to be substantially different from what has been found previously in similar studies on liquid crystal monomers. Dynamic dielectric measurements have probed the different molecular motions in both confinements and how these motions are developed in a way similar to the bulk-dimer. Dielectric results have also proved that the surface-pinned molecular layer (where molecular motions are very restricted) adjacent to the pore-wall is temperature-dependent as already found previously for liquid crystal monomers.

1. Introduction

Liquid crystal dimers are very promising materials, not only because of their technological potential but also on a more fundamental level as they exhibit a range of unusual liquid crystalline behavior. The constituent molecules of such materials are made up of two mesogenic units linked by a flexible spacer, most commonly an alkyl chain. Previously, the mesogenic units were usually calamitic-core moieties, although discotic-core moieties have also been proposed.[1] More recently, combinations of bent-core with calamitic-core moieties or even only bent-core moieties are being explored.[2–6]

At the beginning, one of the most studied topics in liquid crystal dimers was the pronounced dependence of their transitional properties on the length and parity of the flexible spacers (the number of carbon atoms in the alkyl chain), the so-called odd−even effect. Other reported research has been concerned with both fundamental understanding and investigating possible new potential applications. Studies have included the novel alternating and modulated smectic mesophases,[7,8] unusual blue phases,[9] chirality in achiral liquid crystal dimers,[10] biaxial nematics,[2] as well as other nematic mesophases with unusual electro-optical effects,[4] strong flexoelectric properties,[9,11] and materials exhibiting glass-like phenomena.[12]

The structural possibilities for liquid crystal dimers, irrespective of the molecular geometry of the mesogenic groups, can be classified as symmetric (identical mesogenic units) or nonsymmetric (different mesogenic units). Among the symmetric dimers, one of the most studied series is the α,ω-bis(4-cyanobiphenyl-4′-yloxy)alkanes, which can be referred to much more simply by the acronym BCB.O*n*, where *n* stands for the number of carbon atoms in the flexible spacer. Unlike the majority of dimeric series of compounds with spacers having lengths from 3 to 12 carbon atoms, the BCB.O*n* series include compounds having 3−22 methylene units in the flexible spacer, being probably the most extensive series of liquid crystal dimers.[1,7] All compounds belonging to this series are nematogenic, exhibiting pronounced odd−even effects (at least up to 14 methylene units in the spacer) in the transitional properties (melting temperature and both temperature and the entropy change associated with the nematic (N)-to-isotropic (I) phase transition). Even members of the series exhibit higher values than odd compounds, and this fact, in some theoretical approaches,[13–17] has been attributed to the dependence of the energetically favored molecular shapes (*conformers*) on the number of atoms in the flexible spacer. It should be stressed

* Author to whom correspondence should be addressed. Address: Grup de les Propietats Físiques dels Materials (GRPFM), Departament de Física i Enginyeria Nuclear, ETSEIB, Universitat Politècnica de Catalunya, Diagonal 647, 08028 Barcelona, Spain. E-mail: david.orencio.lopez@upc.edu.

[†] Universidad del País Vasco.

[‡] Universitat Politècnica de Catalunya.

[§] University of Southampton.

10.1021/jp9121084
Published on Web 05/24/2010

that the distribution of conformers between the accessible states are temperature-dependent over the range of the mesophase.

Of particular interest in the context of this paper is a simple generic model,[17] which has proved to be valuable in accounting for some experimental results for the BCB.O*n* dimers, such as the odd−even effect and earlier dielectric experiments.[18] On the basis of this model, depending on the parity of the alkyl chain (at least for a number of carbons greater than or equal to 5), the most probable conformers for even dimers exhibit angles between the mesogenic units of 180° (linear conformer) and 71° (bent conformer), while for the odd dimers, the angles are 109° (bent or trans conformer) and 0° (linear or cis conformer). In addition, it is assumed that dimers are binary mixtures of linear and bent conformers, which are able to interconvert as the long-range orientational order changes due to steric effects: the more elongated molecules are, the better accommodation is in a nematic environment. Thus, the difference in properties between even and odd dimers is reflected by the proportion of their corresponding most probable conformers. Relatively recent dielectric experiments on two symmetric dimers of the BCB.O*n* series (BCB.O10 and BCB.O11)[19,20] have evidenced that the above generic model fails to explain all the dielectric measurements. The dielectric behavior of bulk BCB.O11, which is of particular interest for us, can be qualitatively explained by a simple model based on changing populations of cis and trans conformers.[20] Additional theoretical developments of the model were reported by Stocchero et al.[21] a few years ago to improve the quantitative agreement of the model with experiment. More details will be given later in section 3.2.

Complex materials formed by liquid crystals include, among other possibilities, a liquid crystal infiltrated in the porous structure of a nonreactive matrix. Depending on the structure of pores, different effects on the liquid crystal properties are expected to be observed. To investigate confinement−finite size and surface effects on the liquid crystal, pseudo-ordered networks with a certain degree of order such as Nucleopore or Anopore membranes may be used. In such porous materials, nearly parallel cylindrical noninterconnected pores are distributed in a random array perpendicular to the membrane surface.

Most of the work reported for nearly parallel cylindrical geometries has been devoted to low molar mass liquid crystals belonging to the alkylcyanobiphenyls (*n*CBs, where *n* is the number of carbons in the alkyl chain) embedded in Anopore membranes.[22–36] However, for the homologous series of the alkyloxycyanobiphenyls (*n*OCBs, where *n* has the same meaning as in the *n*CBs), the results are very scarce[37–39] and are mainly devoted to specific-heat and dielectric experiments. Even so, some important results concerning the effects of confinement (surface anchoring and finite size effects) on properties have been obtained.

To advance in our previous studies on the *n*OCB-like compounds confined to Anopore membranes, we consider the BCB.O*n* series of liquid crystal dimers, which are the dimers derived from the *n*OCBs. To the best of our knowledge, no studies of liquid crystal dimers confined to Anopore membranes have been reported to date. The present paper describes the first study, using dielectric as well as specific heat measurements, of the effects of the confinement on the molecular alignment at the surface, the surface-induced order and wetting, and molecular dynamics in an odd-symmetric liquid crystal dimer, the nematogenic BCB.O11. For dimers, in addition to the influences experienced by low molar mass liquid crystals, there are likely to be other effects. In particular, it is known that molecular conformations of dimers are influenced by their molecular flexibility. Under such circumstances, it is possible that the restricted cylindrical confinement of 200 nm Anopore membranes will provide an external perturbation high enough to appreciably change the relative populations of bulk conformations. The BCB.O11 liquid crystal dimer seems to be a good model system to study the influence of confinement on the average molecular shape because of its highly flexible alkyl spacer. Also, its dielectric properties have been extensively studied in the bulk state.

The paper is organized as follows. In section 2 we describe the experimental details. In section 3, we present and discuss results concerning the specific heat data through the N-to-I phase transition and dielectric measurements. For the latter, the different molecular motions in the bulk have been previously identified. In section 4, an overall discussion along with the main conclusions focuses on three aspects: molecular alignments in monomers versus dimers, surface-induced order and molecular conformations, as well as the N-to-I phase transition.

2. Experimental Section

2.1. Material. Measurements were undertaken on the odd-symmetric BCB.O11 dimer, the schematic molecular structure of which is

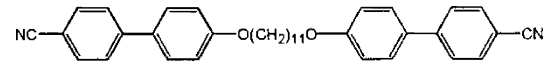

The mesophase sequence on heating from the crystal is N and I. The synthesis of BCB.O11 has already been reported elsewhere.[40,41] The purity was stated to be higher than 99.9%, and no further purification was made.

2.2. Sample Preparation. Anopore membranes consist of a high-purity Al_2O_3 matrix with cylindrical pores of diameter 200 nm, being more or less parallel through their 60 μm thickness. Their large porosity (more than 40%), high surface-to-volume ratio, well-defined pore size, and adequate distribution of pores in the matrix are properties for good slight-restrictive porous materials for confined studies.

As in previous works,[36–39] 200 nm Anopore membranes were cut in disks of about 5 mm diameter and submitted to a previously reported cleaning process.[27] For confined liquid crystal molecular alignments, pore treatment was performed with a chemical surfactant (hexadecyltrimethylammonium bromide (HTBA)) following a procedure described elsewhere.[37] Treated and untreated membranes were immersed in an isotropic bath of BCB.O11 for a period of about 2 h. Filled membranes were carefully dried, removing the excess liquid crystal material from the outer surfaces. Each single disk contained 0.8−0.9 mg of BCB.O11, which supposes an estimated average filling rate of about 85%, similar to that obtained for us in previous studies for other liquid crystals in the same kind of confinement[36–39] and by other authors.[22,24]

2.3. Experimental Techniques. Some experimental techniques such as thermogravimetry using TG Q50 from TA Instruments as well as optical polarized microscopy with an Olympus polarizing microscope equipped with a Linkam TMS-94 temperature controller, were used to check the samples.

Static specific-heat data at constant pressure were obtained through the modulated differential scanning calorimetry (MDSC) technique, using the commercial TA Instruments DSC Q-100, for which extensive details can be found elsewhere.[37,39,42] It is important to realize that, like an alternating current (ac) calorimeter, the MDSC technique, besides providing specific-

heat data, simultaneously gives phase shift data that allow the determination of the coexistence region in weakly first-order transitions. In such cases, experimental conditions were adjusted so that the phase lag ϕ ($\delta = (\pi/2) - \phi$) between the heat flow rate and temperature rate oscillations is effectively zero outside the region of the phase transition, and the imaginary part of the complex specific-heat data is also zero. By calibrating with very precise latent heat data measured for other homologous-compounds from adiabatic calorimetry, it is possible to use the MDSC-technique for quantitative measurements of latent heats of first-order transitions, even if they are weak. Such measurements were performed on cooling from the I-phase down to the N-mesophase and on heating, both at 0.01 K·min^{-1}, with a modulation temperature amplitude of ±0.035 K and a period of 25 s.

Measurements of the complex dielectric permittivity $\varepsilon^*(f) = \varepsilon'(f) - i\varepsilon''(f)$, in the range 10^2 to 1.8×10^9 Hz, were performed using two impedance analysers: the HP 4192A and 4291A. The cell consists of two gold-plated brass electrodes (diameter 5 mm) separated by either 50 μm thick silica spacers for nonconfined samples or about 60 μm thick for the Anopore membrane having confined samples. A modified HP16091A coaxial test fixture was used as the sample holder. It was held in a cryostat from Novocontrol and both temperature and dielectric measurements were computer-controlled.

Bulk samples spontaneously align parallel to the metal electrodes, and thus the component of the dielectric permittivity perpendicular to the probing electric field is easily obtained. The parallel component to the probing electric field, since the material has positive dielectric anisotropy, is obtained by applying a bias electric field. From earlier studies,[20] 30 V bias voltage has proved to be enough to fully align the material along the probing electric field direction. The measuring ac voltage was 0.5 V_{rms} in all cases.

To compare the dielectric permittivities in nonconfined and confined geometries, a rescaling procedure, successfully applied in previous works devoted to monomeric substances,[36,38,39] is used. When the liquid crystal is confined to the membranes, the measured capacity could be attributed to two parallel capacitors: the alumina matrix and the confined liquid crystal. We can deduce an "apparent complex permittivity": $\varepsilon_{ap}=(C_m - C_{al})/pC_0$, where $C_{al} = (1 - p)C_0\varepsilon_{al}$ accounts for the matrix capacity (in this equation, ε_{ap} and C_m are complex quantities; in the studied frequency and temperature ranges, the permittivity of the alumina is nearly constant, and C_{al} is a real quantity), $p = 0.7$ is the porosity, and C_0 is the geometrical capacity of the capacitor. From this value we cannot deduce the liquid crystal permittivity because we cannot propose an equivalent circuit for the pores+liquid crystal system due to the possible inhomogeneity of the filling of the cylindrical pores by the liquid crystal. However, in order to compare the dielectric strengths of the different modes in the bulk and in the confined geometries (both treated and untreated), the residual high-frequency permittivity in the I phase (for the confined case with the above-defined apparent quantities) has been compared, obtaining $\varepsilon_{\infty,bulk}/\varepsilon_{\infty,ap} = 1.3$ for the treated case and $\varepsilon_{\infty,bulk}/\varepsilon_{\infty,ap} \approx 1$ for the untreated one. Assuming that the physical mechanisms contributing to ε_∞, mainly the induced polarization, should not be greatly affected by the confinement, all the data have been rescaled according to these values.

Dielectric measurements were performed on heating and on cooling with different temperature steps being stabilized to ±20 mK.

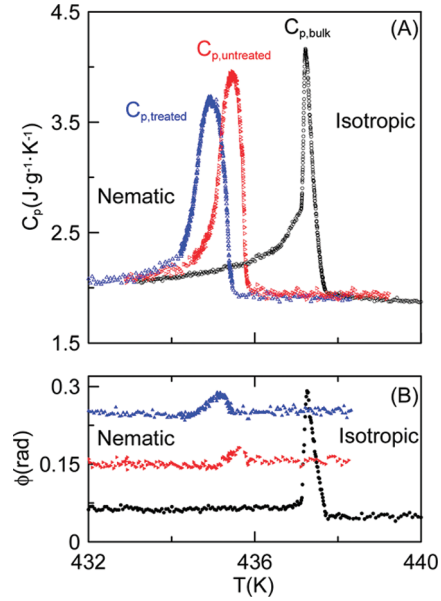

Figure 1. Specific-heat data (A) and ϕ phase shift (B) versus temperature at the N-to-I phase transition for bulk (black symbols) and confined BCB.O11 dimer (red and blue symbols stand for untreated and HTBA-treated confinements, respectively). All the data presented have been obtained on heating.

TABLE 1: Thermal Properties of the N-to-I Transition for Bulk, Untreated, and HTBA-Treated BCB.O11 Dimer[a]

system	T_{NI} (K)	ΔT (K)	$\Delta S_{NI}/R$	$\Delta T_{c.r}$ (K)	ΔC_p(J·g^{-1}·K^{-1})	fwhm
bulk	437.2		1.22	0.71	2.20	0.25
untreated	435.5	−1.7	1.54	0.88	1.99	0.70
treated	434.9	−2.3	1.53	0.95	1.75	0.76

[a] T_{NI} and ΔS_{NI} are temperature and entropy change at the N-to-I phase transition. ΔT is the shift from the bulk. $\Delta T_{c.r}$ is the temperature amplitude of the coexistence region at the N-to-I phase transition. ΔC_p is the difference between the specific-heat maximum and the background at the peak temperature. fwhm is the full width at the half maximum of the specific-heat peak.

3. Results and Discussion

3.1. Specific-Heat Study at the N-to-I Phase Transition. Figure 1A shows the specific-heat data of the BCB.O11 dimer near the N-to-I phase transition as a function of temperature for bulk as well as for confined samples in both treated and untreated Anopore membranes. Compared with the bulk specific-heat data, both treated and untreated confinement experiments showed significant downward shifts in temperature as well as a slight decrease of their apparent heights of the specific-heat peaks. Table 1 reports transition temperatures (T_{NI}) corresponding to the apparent specific-heat maximum and transition temperature shifts (ΔT) from the bulk. It should be stressed from Figure 1A that the confinement in untreated Anopore membranes leads to higher transition temperatures than that in HTBA-treated membranes, similar to results for low molar mass liquid crystals such as the *n*CBs[24] and their homologues *n*OCBs.[37,39] However, both confined samples (untreated and HTBA-treated membranes) exhibit similar broad peaks, with full width at half-maximum (fwhm) 3 times that observed for bulk specific-heat samples (see Table 1). Even so, both confined specific-heat peaks seem to retain the sharp and bulk-like decrease on the I side of the transition. Both facts constitute a substantial difference from what was found for the monomers.[24,37,39]

The specific-heat peak height suppression, due to the confinement, is quantified in Table 1 by the difference between the

specific-heat maximum and the background value at T_{NI} (ΔC_p). In both untreated and HTBA-treated samples, the height suppression seems to be comparable and occurs to a much lesser extent than in the studied *n*OCB compounds.[37,39]

Figure 1B shows the values of the ϕ-shift phase for bulk and confined samples through the N-to-I phase transition. In all cases, a peak in the ϕ-shift phase is observed at the same temperature as that corresponding to the peak for the specific-heat. This feature in ϕ at the phase transition seems to be associated with the existence of latent heat at the transition and usually is used to obtain the coexistence region of the phase transition. The temperature amplitude of the coexistence region (ΔT_{cr}), given in Table 1, increases for confined samples (HTBA-treated exhibits the highest value), and, in fact, it is the first time that a liquid crystal confined in HTBA-treated Anopore membranes shows a ϕ-shift phase peak at the N-to-I phase transition and so allows the coexistence region to be determined.

As for the latent heat associated with the N-to-I phase transition, it is known from the literature[1] that the value for the bulk is about 4.5 kJ·mol^{-1} (or an entropy change in units of the R-constant of about 1.25). It is evident that this phase transition is of first order with a relative high latent-heat similar in magnitude to what is observed for the *n*OCB compounds at the smectic A-to-I phase transition. Determinations of enthalpy changes are easily attainable by means of standard DSC experiments. Our calculated values following the MDSC procedure,[37,42] either for bulk or for confined samples, expressed as the entropy change in units of R, are presented in Table 1. It should be stressed that both untreated and HTBA-treated entropy changes are higher than that reported for the bulk. This fact appears to be surprising and will be discussed later.

3.2. Dielectric Study. ***3.2.1. Theoretical Background and Dielectric Spectra Analysis.*** The frequency-dependent dielectric permittivity components (director parallel, $\varepsilon_{\parallel}(\omega)$, and perpendicular, $\varepsilon_{\perp}(\omega)$, to the probing electric field), can be related to the time correlation functions for the molecular dipoles through the Laplace transform, using a suitable model. A general theory for the dielectric relaxation of rigid dipolar molecules in nematic fluids has been developed by Nordio et al.[43] assuming for the molecular dynamics the rotational diffusion model in the presence of a nematic potential. For each configuration, two modes are expected whose dielectric strengths and relaxation frequencies depend on the values of the molecular dipole and its direction with respect to the long molecular axis, the molecular anisotropy, and the orientational order parameter. The relative strengths of these relaxations can be calculated using the Maier and Meyer equations. For compounds with dipole moments mostly along the long molecular axis, the main contribution to the parallel component is due to the molecular reorientation about the short axis. Its dielectric strength, among other factors, depends directly on the order parameter, showing an increase as the order increases. The associated relaxation frequency, together with the usual dependence on the viscosity, is greatly influenced by the order parameter, because of the increase of the nematic potential. As a consequence, the relaxation frequency should decrease rapidly when temperature decreases.

Some years ago, Stocchero et al.[21] proposed a theoretical model for nematogenic liquid crystal dimers, which in essence considers that the dipole correlation function is modulated by both the overall rotational motions of the rigid mesogens and the conformational changes of the flexible chain connecting them. Calculations of both the parallel and perpendicular components of the static dielectric permittivity are in quite good agreement with experimental measurements[20] showing that both components decrease with decreasing temperature. This calculated behavior, using the model with a full torsional potential for the alkyl spacer, is due to the fact that the trans-conformer population increases with order and, in addition, the conformers become more extended, i.e., the angles between the mesogenic units are higher than 109° in contrast with that previously predicted by the rotational isomeric state (RIS) model.[17] In the model, for sufficiently large-order parameters, the mesogenic units tend to be aligned parallel to the director, as shown in Figure 2. Each one of the states shown corresponds to a shallow minimum, and they represent the stable states of the dimer. From the shape of the potential of mean torque, Stocchero et al.[21] suggest that only the independent π-rotations of each rigid unit should be taken into account because they correspond to the crossing of the saddle points. The simultaneous rotations of the two rigid units (i.e., $a \leftrightarrow d$ and $b \leftrightarrow c$ in Figure 2) can be excluded because they are associated with the passage through a potential maximum, which has too large an activation energy to produce a significant transition rate.

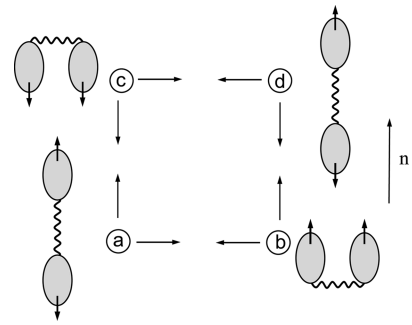

Figure 2. Schematic representation of the four stable states for symmetric dimers, according to Stocchero et al.'s[21] theoretical model.

Let us consider the model[21] of Stocchero et al. to be applied to symmetric dimers, such as the BCB.O11, case (iii) in the quoted paper. There are two identical dipolar moieties (associated with the terminal cyanobiphenyl groups of the BCB.O11), and the parallel component of the dielectric permittivity is predicted to exhibit one main dielectric relaxation at low frequencies, denoted hereafter as the m_1-mode. It is also predicted that, although the frequency decreases as in conventional monomers, the dielectric strength diminishes when temperature decreases as a consequence of the lowering of the cis-conformer population because trans conformers do not have a net longitudinal dipole moment.

Experimental determinations of the real and imaginary parts of the permittivity in the parallel and perpendicular alignments are reproduced in Figure 3 as a function of frequency for both the N mesophase and the I phase. One of the major difficulties in the spectra analysis arises when the different relaxation modes occur closely spaced in the frequency domain, in such a way that dielectric loss peaks appear partially superimposed. In addition, often the spectral shape of each mode does not correspond to a pure exponential Debye relaxation, and the analysis should be performed using the empirical Havriliak−Negami (H−N) function, given as

$$\Delta\varepsilon_k(\omega) = \frac{\Delta\varepsilon_k}{(1 + (i\omega\tau_k)^{\alpha})^{\beta}} \quad (1)$$

where $\Delta\varepsilon_k$ is the dielectric strength, τ_k is the relaxation time, the subscipt k labels each relaxation process, α and β are

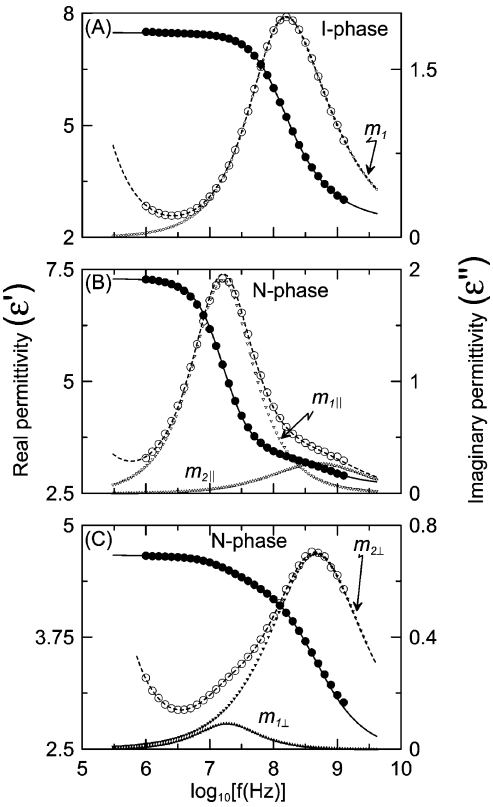

Figure 3. Frequency dependence of the dielectric permittivity of bulk BCB.O11 dimer, in the I phase ($T = 443.15$ K) (A) and in the N phase ($T = 423.15$ K) (B,C). Dashed and solid black lines are fittings according to eq 1. Open and filled triangle lines represent deconvolution into elementary modes m_1 and m_2. For simplicity, the direct current (dc) conductivity contribution is not drawn, but it is considered in the fittings.

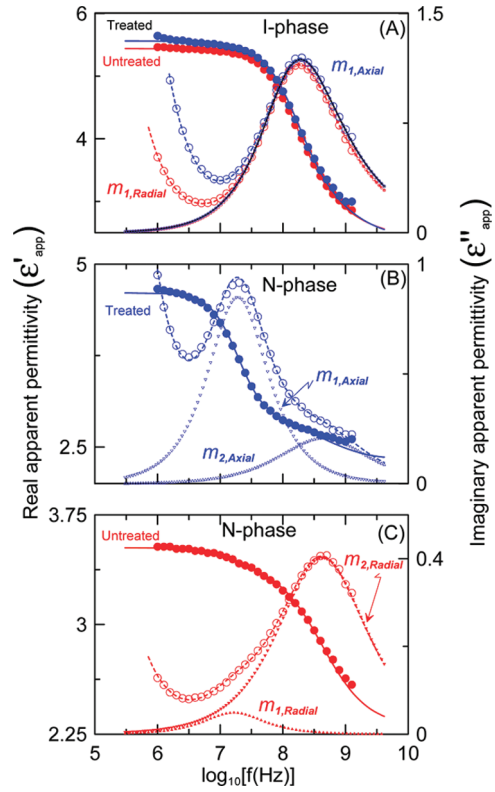

Figure 4. Frequency dependence of the dielectric permittivity of HTBA-treated (blue lines and symbols) and untreated (red lines and symbols) BCB.O11 dimer, in the I phase ($T = 443.15$ K) (A) and in the N phase ($T = 423.15$ K) (B,C). Dashed and solid lines are fittings according to eq 1. Open and filled triangle lines represent deconvolution into elementary modes m_1 and m_2. For simplicity, the dc conductivity contribution is not drawn, but it is considered in the fittings.

parameters describing the shape (symmetry and width), and $\alpha = \beta = 1$ corresponds to Debye relaxation.

Figure 3A shows, as an example, the real and imaginary parts of the dielectric permittivity measured as a function of frequency in the I-phase at 443.15 K. The results were fitted to only one mode ($\alpha = 0.93$; $\beta = 0.65$). Due to the lack of order, this contribution could be attributed to a concerted rotation of the whole dimer, mainly in the cis conformation, denoted as the m_1 mode.

Figure 3B shows typical dielectric relaxation curves for the real and imaginary parts as a function of frequency in the N-mesophase (parallel alignment with bias electric field) at 423.15 K. The results were fitted to two relaxation processes. The low-frequency relaxation (Debye-like) is identified with the change in the orientation of a single mesogenic group via changes in the conformational state of the flexible spacer of the dimer (hereafter referred to as end-over-end motion of the dipolar groups) denoted the $m_{1\|}$ mode. This mode contributes to the dielectric response to a different extent, depending on the population of cis and trans conformers because the latter have a null net dipole moment. The high-frequency relaxation ($\alpha = 0.74$; $\beta = 1$) is suggested to be attributed to precessional motions of the dipolar groups and is assumed to be comparable in cis and trans conformers (denoted as the $m_{2\|}$ mode).

Figure 3C shows, as an example, both components (real and imaginary parts) of the dielectric permittivity in the N mesophase (with the sample in perpendicular alignment) at 423.15 K. Two relaxation modes can also be observed. The low-frequency mode appears at a frequency similar to that found in parallel alignment but only with a few percent of the strength measured for the latter. The authors attribute this mode to a nonperfect perpendicular alignment of the director (for coherence we denote this mode as $m_{1\perp}$ and it is Debye-like). The high frequency mode, the most prominent in such a perpendicular alignment ($\alpha = 0.77$; $\beta = 1$), is believed to be caused by precessional motions of the dipolar mesogenic units, contributing both cis and trans conformers (denoted as the $m_{2\perp}$ mode).

As explained in section 2.3, a temperature-and-frequency-dependent apparent complex dielectric permittivity ($(\varepsilon^*_{app}(T,\omega))$) for the BCB.O11 dimer confined to Anopore membranes rescaled using the R factors ($R_{untreated} = 1$; $R_{treated} = 1.3$) is obtained. Figure 4 shows the typical profiles (real and imaginary parts) of the apparent dielectric permittivity in the I-phase (Figure 4A) as well as in the N-mesophase, for untreated (Figure 4B) and treated (Figure 4C) Anopore membranes. It should be pointed out that, by comparing both Figures 3 and 4, BCB.O11 confined to HTBA-treated and untreated Anopore membranes exhibits parallel and perpendicular bulk-like alignments, respectively. Parallel bulk-like alignment means that the molecules of BCB.O11 are mostly aligned tangential to the pore cylindrical axis, and so the confinement of BCB.O11 to HTBA-treated membranes leads to axial alignment. Perpendicular bulk-like alignment means that the molecules of BCB.O11 are mostly aligned perpendicular to the pore cylindrical axis. This kind of alignment can be denoted as radial and the so-called[24,37,44] planar polar (PP) and planar radial (PR) configurations would be compatible with such an alignment. Escaped radial (ER) or escaped radial with point defects (ERPD) configurations would represent mixed behaviors between parallel bulk-like and perpendicular bulk-like alignments. Figure 4B,C seems to

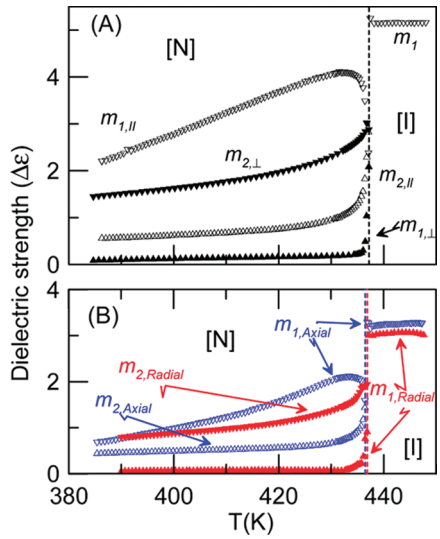

Figure 5. Dielectric strength versus temperature of the different elementary contributions for bulk (A) and confined (B) BCB.O11 dimer. Blue and red symbols correspond to axial and radial confinements, respectively.

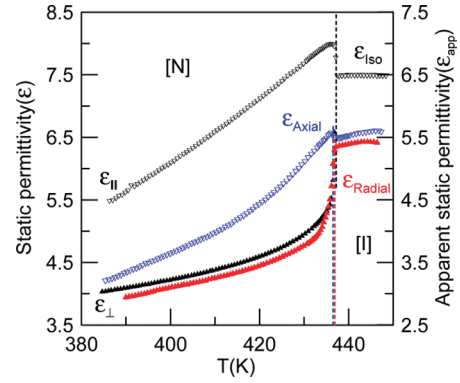

Figure 6. Static dielectric permittivity of bulk (left *y*-axis and black symbols) and apparent static dielectric permittivity of confined BCB.O11 dimer (right *y*-axis) versus temperature in the I and N phases. Blue and red symbols correspond to axial and radial confinements, respectively.

discard both mixed-configurations for the BCB.O11 confined to Anopore membranes. Hereafter, the untreated and HTBA-treated membrane results will be referred to as radial and axial, respectively, both irrespective of the phase (either I or N).

Let us analyze in detail the dielectric results displayed in Figure 4 by comparing with the results established for bulk dimer BCB.O11 (see Figure 3). Figure 4A shows both components (real and imaginary parts) of the apparent dielectric permittivity in the I-phase at 443.15 K. The results for both HTBA-treated (axial alignment) and untreated (radial alignment) were similarly fitted, according to the procedure followed for the bulk, to one mode ($\beta = 0.65$ and $\alpha = 0.91$ for axial confinement; $\beta = 0.67$ and $\alpha = 0.93$ for radial confinement). Both modes are denoted as $m_{1,Axial}$ and $m_{1,Radial}$.

Figure 4B shows both components (real and imaginary parts) of the apparent dielectric permittivity (axial confinement) in the N-phase at 423.15 K. Our analysis reveals two adjacent processes identified as the m_1 mode (denoted as $m_{1,Axial}$, which is Debye-like) and the m_2 mode (denoted as $m_{2,Axial}$ in which $\beta = 1$ and $\alpha = 0.77$).

Figure 4C shows both components (real and imaginary parts) of the apparent dielectric permittivity (radial confinement) in the N-mesophase at 423.15 K. The radial configuration spectra, following the bulk-procedure is resolved into two modes: $m_{1,Radial}$ (Debye-like) associated with the end-over-end motion of the dipolar mesogenic groups, the consequence of a nonperfect perpendicular alignment, and $m_{2,Radial}$ ($\alpha = 0.78$, $\beta = 1$) due to the precessional motion of the dipolar mesogenic groups of cis and trans conformers.

Although in Figure 4 the only the spectra in the 10^6 to 1.8×10^9 Hz frequency range have been shown, measurements down to 10^2 Hz were also performed. These measurements did not reveal the existence of any additional process, excluding some low frequency spurious effects associated with the electrode polarization or Maxwell−Wagner effect.

3.2.2. Temperature Dependence of the Dielectric Behavior. Figure 5A shows the temperature dependence of the dielectric strength data for all the aforementioned relaxation modes in the bulk dimer in both alignments. In parallel alignment, the dielectric strength of the $m_{1||}$ mode ($\Delta\varepsilon_{m1||}$) increases on entering the N-mesophase from the I-phase, exhibiting a maximum close to the N-to-I phase transition as it was previously reported.[20] This fact is explained as a slight stabilization of the cis-conformer population. However, when the order increases in the N-mesophase, which means that temperature decreases, the population of strongly polar cis conformers diminishes abruptly. It should be stressed that the evolution of $\Delta\varepsilon_{m1||}$ with temperature is strongly dependent on the molecular conformation of the dimer unlike what happens for $\Delta\varepsilon_{m2||}$, which abruptly decreases on entering the N-mesophase stabilizing in a nearly constant value at lower temperatures.

In perpendicular alignment, the dielectric strength of the low frequency relaxation, denoted as the $m_{1\perp}$ mode, could be considered as a spurious contribution due to a nonperfect perpendicular alignment. The most prominent contribution comes from the high-frequency relaxation ($m_{2\perp}$ mode). Its dielectric strength ($\Delta\varepsilon_{m2\perp}$) evolves with temperature, to a certain extent, similar to $\Delta\varepsilon_{m2||}$, as is expected.

Figure 5B shows the temperature dependence of the dielectric strength data of the different relaxation modes in both the axial and radial confinements. At first glance, there is a clear correspondence in the evolution with temperature of the dielectric strength data between the bulk-parallel and the axial confinement on one hand and between bulk-perpendicular and radial confinement on the other. It could be suggested that, in the axial confinement, cis conformers convert into trans conformers as the temperature decreases in the N-mesophase.

In the I-phase, there exists a small difference in the strength data associated with the same molecular mode when axial and radial confinements are compared. In fact, $\Delta\varepsilon_{m1,Axial}$ data is higher than $\Delta\varepsilon_{m1,Radial}$ data, as it has also been observed for monomeric *n*OCBs,[37–39] and the difference tends to increase at higher temperatures in the I-phase.

The temperature dependence of the static permittivity for bulk in both alignments, parallel and perpendicular, along with the apparent static dielectric permittivity for axial and radial confinements is shown in Figure 6. These quantities have been calculated by adding the corresponding dielectric strengths (Figure 5) plus the high-frequency limit (in each case, ε_∞, $\varepsilon_{\infty,Axial}$, and $\varepsilon_{\infty,Radial}$, for bulk, axial, and radial, respectively) as deduced from the fittings of the complex dielectric permittivity. Bulk data (refer to the left *y*-axis of Figure 6) and confinement data (refer to the right *y*-axis of Figure 6) are displayed on the same absolute scale to facilitate comparison. By comparing the parallel component of the static permittivity ($\varepsilon_{||}$) with the apparent static permittivity for axial confinement (ε_{axial}), many similarities can be found. In particular, for both, a maximum in the N-

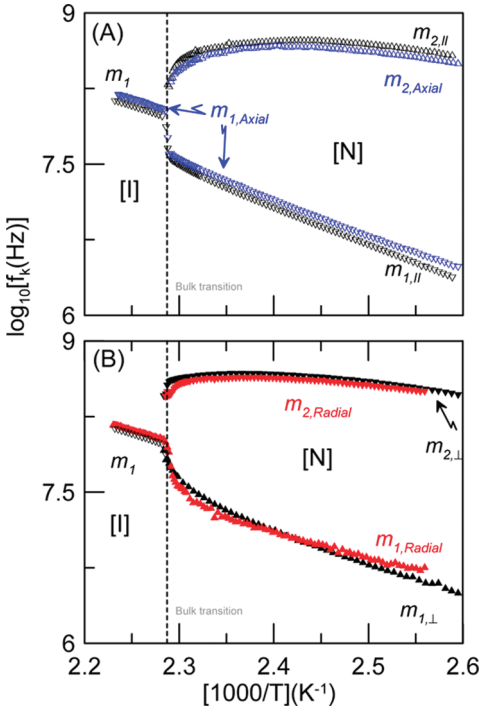

Figure 7. Arrhenius plot of the relaxation frequencies (f_k) of the different elementary contributions for bulk-parallel and axial confinement (A) as well as bulk-perpendicular and radial confinement (B) of BCB.O11 dimer. Black, blue, and red symbols correspond to bulk, axial, and radial confinements, respectively.

mesophase, close to the N-to-I phase transition is observed. Likewise, both magnitudes decrease with temperature, although not in the same way; an important fact that will be discussed later. It should be stressed that both $\varepsilon_{||}$ or ε_{axial} are mainly due to π-rotations of each mesogenic dipolar unit of the dimer (m_1 mode), also denoted as end-over-end motions of the mesogenic units. Likewise, in the N-mesophase, the temperature dependence of $\varepsilon_{\perp}$ and ε_{radial} appears to not only be similar to one another, but also to the dielectric strength of the m_2 mode ($\Delta\varepsilon_{m2,\perp||}$ and $\Delta\varepsilon_{m2,Radial}$). Therefore, it could be concluded that ε_{radial} and $\varepsilon_{\perp}$ are mainly due to precessional motions of the dipolar groups of the dimer. As for the I-phase, both ε_{axial} and ε_{radial} increase with temperature, at least, for about 10 K above their respective N-to-I phase transition temperatures. For temperatures higher, both magnitudes seem to saturate, displaying a similar trend that the static permittivity of the bulk (ε_{iso}).

Figure 7A,B shows, in an Arrhenius plot, the temperature dependence of the characteristic relaxation frequency data (bulk alignments and confined configurations) associated with each mode for both the N and I phases. Figure 7A corresponds to bulk-parallel and axial confinement, and Figure 7B corresponds to bulk-perpendicular and radial confinement. Both figures are of great importance to get comparative information about the molecular mobility in both confinements. In the I-phase, the mobility of the molecules in both confinements seem to be nearly the same, but they are slightly faster than in the bulk. However, it is important to remember that there exists a certain difference between both sets of strength data (about a 5%). This means that the number of molecules per unit of volume whose dipolar mesogenic units are moving is less in radial than in axial confinement. When the N-to-I phase transition occurs, end-over-end motions of the dipolar mesogenic units in the axial confinement remain faster than those in bulk-parallel, but precessional motions of dipolar groups are slightly slower. In the case of radial confinement, these precessional motions are also slightly slower than those in bulk-perpendicular.

From Figure 7, it seems to be that the Arrhenius behavior is satisfied in the I and N phases for both axial and radial configurations as well as for both bulk-alignments (parallel and perpendicular), at least, for the main molecular modes. It should be stressed that, in the I-phase, the activation energy of m_1 mode is about 60 kJ·mol^{-1} regardless of bulk or both confinements, either axial or radial. In the N-mesophase, no differences are also observed on the activation energies of the m_1 mode between bulk-parallel and axial confinement, being about 70 kJ·mol^{-1}. Activation energies of the main molecular mode in the N-mesophase for bulk-perpendicular and radial confinement (m_2 mode) are nearly identical between them, although they are more than 1 order of magnitude (about 5 kJ·mol^{-1}) lower than those obtained for m_1 mode.

4. Overall Discussion and Concluding Remarks

4.1. Molecular alignments in dimers vs monomers. It has been known for some time that there are difficulties in achieving homeotropic alignments on metallic surfaces for symmetric BCB.O*n* dimers.[19,20] For BCB.O11 such a homeotropic alignment can be successfully obtained by applying a bias electric field. On the *n*CB or *n*OCB monomers, at least for alkyl chains of no more than 9 or 10 carbons, homeotropic alignment is spontaneously achieved.

When the surface to be anchored to the liquid crystal molecules is alumina, as in the case of liquid crystal confinement to Anopore membranes, the situation changes drastically. For *n*CB and *n*OCB monomers with *n* no longer than 9 or 10, molecules spontaneously anchor to the hydrophilic alumina surface in a planar alignment giving rise to the so-called axial confinement. However, the surface anchoring perpendicular to the pore wall is enhanced as the number of carbons of the alkyl chain increases.[33,39] It is known from old results on 8CB that the hydrophilic polar groups (−CN) are adsorbed on a hydrophilic surface, and the hydrophobic alkyl chain tails are tilted at about 70° from the surface normal.[45] This configuration favors planar alignment of 8CB molecules on alumina surfaces.[24,36] As the chain length increases in the *n*CB series, the alkyl chain tilt angle from the surface normal tends to be smaller favoring homeotropic anchoring.[33] This simplified picture can be completely extended to the *n*OCB compounds with very minor modifications due to the presence of oxygen in the alkyl chain tail of the molecule.[37,39] However, if one wants to get hometropic alignment irrespective of the length of the alkyl/alkyloxy chain, surface treatment with an appropriate chemical surfactant must be made. There are many possibilities, and one of the most extensively used was the L-α-lecithin despite its relatively complex molecular structure.[46] The authors of the current paper prefer to use HTBA, which has a strong polar headgroup easily adsorbed by the hydrophilic alumina surface and a long enough alkyl chain along the surface normal. It has been reported by us[36–39] how well the alkyl chain of HTBA promotes homeotropic alignment on *n*OCB molecules onto alumina surfaces.

Let us now consider what happens when BCB.O*n* dimers are confined to the hydrophilic pores of Anopore membranes, and especially the case of BCB.O11. Our results show that, in untreated Anopore membranes, BCB.O11 dimer molecules are arranged in a radial configuration (homeotropic alignment to the alumina surface). Although this fact could be an inconvenience, it should not be surprising. However, what is found when BCB.O11 dimer molecules are confined to HTBA-treated Anopore membranes is really something unexpected: the

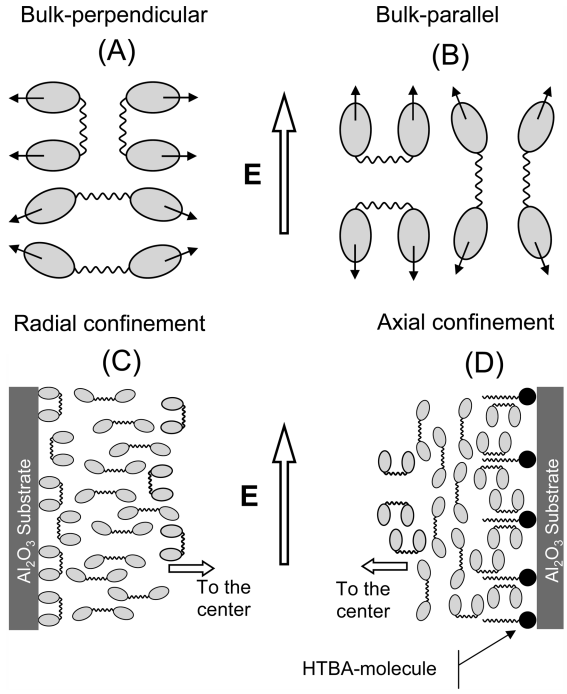

Figure 8. Schematic representation of bulk-perpendicular (A) and bulk-parallel (B) molecular alignments for BCB.O11 dimer. Schematic picture of the dimer arrangement onto nontreated (C) and HTBA-treated (D) alumina substrates. The arrow stands for the probing electric field.

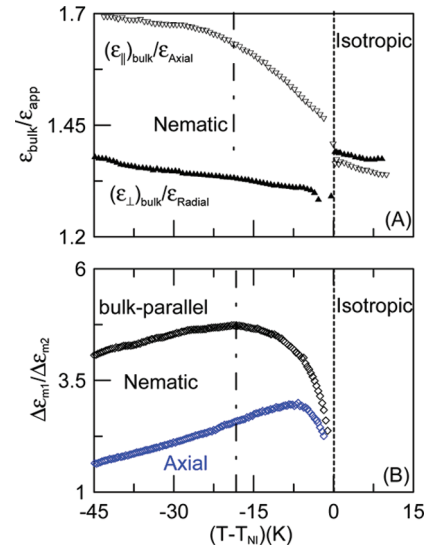

Figure 9. (A) The ratio of the static permittivity bulk data over apparent static permittivity data for axial (black-down triangles) as well as radial (black triangles) alignments versus $(T - T_{NI})$. (B) The ratio of the dielectric strength data of the m_1 mode over dielectric strength data of the m_2 mode for bulk-parallel (black symbols) and axial confinement (blue symbols).

molecules are arranged in an axial configuration. In Figure 8, a possible explanation is suggested. First of all, when we speak of bulk-perpendicular alignment, the BCB.O11 molecules in cis or trans conformation are thought to be arranged as shown in Figure 8A, while for bulk-parallel alignment the schematic view is displayed in Figure 8B. The question now is how HTBA-treated alumina surface could promote axial confinement. HTBA molecules are thought to be arranged with the polar head adsorbed by the alumina surface and the alkyl tail along the normal to the surface (Figure 8D). In order to promote a sort of alignment similar to bulk-parallel, it would be required that those molecules closer to the alumina surface must be cis conformers instead of trans conformers, as it is schematized in Figure 8D. For radial confinement, this possibility is also shown in Figure 8C. It should be stressed that the dimer is introduced into the pores in the I-phase, and the model depicted in Figure 8C,D would require that, from the mixture of conformers, only those in cis conformation would be preferably arranged close to the wall, at least, in the case of axial confinement.

4.2. Surface-Induced Order and Molecular Conformations. One of the most striking effects of confinement on liquid crystal monomers is the effect of the surface that favors anisotropic interactions leading to an orientationally ordered layer near the surface. Dielectric results clearly show how the extension of this ordered layer is revealed to be temperature-dependent and how the molecules of liquid crystal monomers, out of this layer, reorient in a similar way as in the bulk.

Liquid crystal dimers are more complex than monomers, but under cylindrical confinement, exhibit a comparable behavior. To start with, confined liquid crystal dimer molecules move in a similar way as in the bulk (see Figure 7), because the energy barrier hindering the molecular motions is nearly the same. End-over-end motions of the dipolar mesogenic units are revealed to be faster than that for the bulk, but it should be remembered that in certain liquid crystal monomers under cylindrical confinement,[36,38] reorientations around the short axis are found to be faster, as well.

As for the surface-pinned molecular layer, at a first glance, there seem to exist serious differences with respect to liquid crystal monomers. In Figure 9A, the ratio of bulk-parallel component $\varepsilon_{||}$ over ε_{Axial} as well as bulk-perpendicular component $\varepsilon_{\perp}$ over ε_{Radial} as a function of $(T - T_{NI})$ are shown. Such a figure clearly shows, in the N-mesophase, how $(\varepsilon_{\perp})_{Bulk}/\varepsilon_{Radial}$ monotonically increases as temperature decreases, as it has always been found for liquid crystal monomers.[37,39] For these compounds, this fact has been explained as being due to the existence of a surface-pinned molecular layer (where the molecules exhibit very restricted molecular motions), the extension of which increases as temperature decreases. The same explanation can be suggested for liquid crystal dimers but, could it explain the overall behavior exhibited in Figure 9A? In the I-phase, $(\varepsilon_{\perp})_{Bulk}/\varepsilon_{Radial}$ decreases as temperature increases, but tends to saturate at about 7 K above T_{NI}, a fact never observed for liquid crystal monomers. This singular feature is also observed for $(\varepsilon_{||})_{Bulk}/\varepsilon_{Axial}$. Both facts are apparently not consistent with the temperature-dependence of the surface-pinned molecular layer, that is to say, it seems that, from a certain temperature, the extension of the layer ceases to be temperature dependent.

Let us now consider in Figure 9A, the trend with temperature of the ratio $(\varepsilon_{||})_{Bulk}/\varepsilon_{Axial}$ in the N-mesophase. It is observed how $(\varepsilon_{||})_{Bulk}/\varepsilon_{Axial}$ increases as temperature decreases, as has been usually found for liquid crystal monomers. However, at about 20 K below T_{NI}, the slope clearly changes, a fact never observed for liquid crystal monomers. Again, it seems that the temperature dependence of the surface-pinned molecular layer fails at a certain temperature.

Figure 9B shows the ratio $\Delta\varepsilon_{m1}/\Delta\varepsilon_{m2}$ as a function of $(T - T_{NI})$ for both the bulk-parallel and the axial confinement. The absolute value of this ratio and its trend with temperature gives information of the relative proportion of cis conformers, which contribute to the $\Delta\varepsilon_{m1}$, over the mixture of conformers, which contribute to the $\Delta\varepsilon_{m2}$. In the N-mesophase, during the first 20 K below phase transition, cis conformers in the bulk contribute

to $\Delta\varepsilon_{m1}$ in a greater proportion than in the axial case. Our explanation consists in considering two effects: (i) the conversion cis-to-trans conformers and (ii) the number of molecules becoming adsorbed onto the surface-pinned molecular layer. Both effects contribute to lowering ε_{Axial} as the temperature decreases. However, in bulk-parallel, only one of these effects (conversion cis-to-trans) has a role in decreasing $(\varepsilon_{||})_{Bulk}$ with temperature. At about 15−20 K below T_{NI}, the trend of the ratio $(\Delta\varepsilon_{m1}/\Delta\varepsilon_{m2})$ is stabilized in both the bulk and the axial confinement, simulating that the extension of the surface-pinned molecular layer does not progress as temperature decreases. However, what actually happens is that many more trans conformers than cis conformers join the surface-pinned molecular layer in such a way that the reduction of the static permittivity (ε_{Axial}) with decreasing temperature slows. This suggestion is supported by the fact that, in Figure 9B, both sets of $(\Delta\varepsilon_{m1}/\Delta\varepsilon_{m2})$ data are nearly parallel; apparently, it is as if the extension of the surface-pinned molecular layer ceases to increase as the temperature decreases, but actually, the layer continues to adsorb molecules (trans conformers) but they do not contribute to $\Delta\varepsilon_{m1}$. The cis conformers outside the layer, which contribute to $\Delta\varepsilon_{m1}$, are in much smaller proportion than in bulk-parallel, but it seems that they undergo the cis-to-trans conversion to the same extent.

The above argument can also be used to explain the saturation of both $(\varepsilon_{\perp})_{Bulk}/\varepsilon_{Radial}$ and $(\varepsilon_{||})_{Bulk}/\varepsilon_{Axial}$ at about 7 K above T_{NI}. As suggested in the preceding section 4.1, cis conformers would seem to be more predisposed to be arranged close to the pore wall in such a way that, just above T_{NI}, the outer limit of the layer is formed by a mixture of conformers, which leave the layer as temperature increases. At the beginning and up to about 7 K above T_{NI}, the number of cis conformers that leave the layer increases the value of ε_{Axial} and ε_{Radial}, but progressively, when more trans conformers leave the layer than cis conformers, both values of the apparent static permittivity tend to saturate.

Finally, from specific-heat as well as dielectric measurements, no evidence of orientational wetting (strongly induced nematic order) in the I-phase just above the N-to-I phase transition, neither in axial nor in radial confinements, is observed. It is important to realize that the orientational wetting in liquid crystal monomers is a phenomenon that is hardly observed in surface-treated Anopore membranes (radial confinement) and, to a lesser extent, for untreated membranes (axial confinement).[22,37,39]

4.3. The N-to-I Phase Transition. As for the N-to-I phase transition, Figure 1 allows us to observe that, unlike what happens in liquid crystal monomers (the most studied *n*CB and *n*OCB), the specific-heat peak at the phase transition corresponding to the radial confinement ($C_{p,untreated}$) is at higher temperatures than the axial one ($C_{p,treated}$). The authors ignore whether this singular fact will be ordinary in confined liquid crystal dimers, but it should be stressed that the relative positions in the temperature of the specific-heat peaks sorted from lowest to highest temperatures, i.e., $C_{p,treated}$, $C_{p,untreated}$, and $C_{p,bulk}$ are identical to what is found for liquid crystal monomers confined to Anopore membranes. It is the type of confinement that is obtained in HTBA-treated and untreated Anopore membranes that is actually inverted.

It is important to realize that the static dielectric behavior of the BCB.O11 dimer in bulk and in confined configurations exhibit, either in Figure 6 or in Figure 7, a certain difference in relation to the N-to-I phase transition temperatures. Although the value from bulk is comparable to that obtained from specific-heat gathered in Table 1, the other two are rather different. Even so, depression of the axial transition temperature with respect to the radial and the latter with respect to the bulk are maintained as is observed from specific heat results (see Table 1 and Figure 1).

Taking into account specific-heat measurements alone, the confinement of liquid crystal dimers, at least to be valid for BCB.O11, to 200 nm Anopore membranes, either axial or radial, seems to affect the specific-heat peak morphology to a lesser extent than for liquid crystal monomers. However, it should be stressed that the latent heat of BCB.O11 associated with the transition is nearly 3 times higher than that observed for the usually measured monomers.[22,24,37,3947] The authors are unaware if the relatively strong character of the first-order phase transition could cause this singular fact. Other liquid crystal dimers with weaker N-to-I phase transitions should be considered in the near future.

Another intriguing fact refers to the entropy changes (ΔS_{NI}) at the phase transition. As commented previously, both confinements exhibit comparable ΔS_{NI} of about 20% higher than for the bulk. For the studied liquid crystal monomers[22,24,37,3949] confined to Anopore membranes, ΔS_{NI} tends to be lower in confined than in bulk samples. It seems that the increment in the ΔS_{NI} value for confined dimers reinforce the idea that the I phase is richer in trans conformers.

Acknowledgment. The authors are grateful for financial support from the MICINN (projects MAT2009-14636-C03-02,03). The authors also acknowledge the recognition as an "emergent research group" (AGAUR-2009-SGR-1243) from the Generalitat de Catalunya Government.

References and Notes

(1) Imrie, C. T., Luckhurst, G. R. Liquid Crystal Dimers and Oligomers. In *The Handbook of Liquid Crystals: Low Molecular Weight Liquid Crystals*; Demus, D., Goodby, J. W., Gray, G. W., Spiess, H. W. ,Vill, V., Eds.; Wiley-VCH: Weinheim, Germany, 1998; Vol. 2B, Chapter X, p 801.

(2) Yelamaggad, C. V.; Prasad, S. K.; Nair, G. G.; Shashikala, I. S.; Rao, D. S. S.; Lobo, C. V.; Chandrasekhar, S. *Angew. Chem., Int. Ed.* **2004**, *43*, 3429.

(3) Lagerwall, J. P. F.; Giesselmann, F.; Wand, M. D.; Walba, D. M. *Chem. Mater.* **2004**, *16*, 3606.

(4) Tamba, M. G.; Kosata, B.; Pelz, K.; Diele, S.; Pelzl, G.; Vakhovskaya, Z.; Kresse, H.; Weissflog, W. *Soft Matter* **2006**, *2*, 60.

(5) Umadevi, S.; Sadashiva, B. K.; Shreenivasa Murthy, H. N.; Raghunathan, V. A. *Soft Matter* **2006**, *2*, 210.

(6) Umadevi, S.; Sadashiva, B. K. *Liq. Cryst.* **2007**, *34*, 673.

(7) Imrie, C. T.; Henderson, P. A. *Chem. Soc. Rev.* **2007**, *36*, 2096.

(8) Sepelj, M. S.; Baumeister, U.; Diele, S.; Nguyen, H. L.; Bruce, D. W. *J. Mater. Chem.* **2007**, *17*, 1154.

(9) Coles, H. J.; Pivnenko, M. N. *Nature* **2005**, *436*, 997.

(10) Takanishi, Y.; Toshimitsu, M.; Nakata, M.; Takada, N.; Izumi, T.; Ishikawa, K.; Takezoe, H. *Phys. Rev. E* **2006**, *74*, 051703.

(11) Ferrarini, A.; Greco, C.; Luckhurst, G. R. *J. Mater. Chem.* **2007**, *17*, 1039.

(12) Attard, G. S.; Imrie, C. T. *Chem. Mater.* **1992**, *4*, 1246.

(13) Emsley, J. W.; Luckhurst, G. R.; Shilstone, G. N. *Mol. Phys.* **1984**, *54*, 1023.

(14) Ferrarini, A.; Luckhurst, G. R.; Nordio, P. L.; Roskilly, S. J. *J. Chem. Phys.* **1994**, *100*, 1460.

(15) Luckhurst, G. R. *Mol. Phys.* **1994**, *82*, 1063.

(16) Luckhurst, G. R.; Romano, S. *J. Chem. Phys.* **1997**, *107*, 2557.

(17) Ferrarini, A.; Luckhurst, G. R.; Nordio, P. L.; Roskilly, S. J. *Chem. Phys. Lett.* **1993**, *214*, 409.

(18) Furuya, H.; Okamoto, S.; Abe, A.; Petekidis, G.; Fytas, G. *J. Phys. Chem.* **1995**, *99*, 6483.

(19) Bauman, D.; Wolarz, E.; Bialecka-Florjanczyk, E. *Liq. Cryst.* **1999**, *26*, 45.

(20) Dunmur, D. A.; Luckhurst, G. R.; de la Fuente, M. R.; Diez, S.; Pérez-Jubindo, M. A. *J. Chem. Phys.* **2001**, *115*, 8681.

(21) Stocchero, M.; Ferrarini, A.; Moro, G. J.; Dunmur, D. A.; Luckhurst, G. R. *J. Chem. Phys.* **2004**, *121*, 8079.

(22) Iannacchione, G. S.; Finotello, D. *Phys. Rev. Lett.* **1992**, *69*, 2094.

(23) Crawford, G. P.; Ondris-Crawford, R.; Zumer, S.; Doane, J. W. *Phys. Rev. Lett.* **1993**, *70*, 1838.

(24) Iannacchione, G. S.; Finotello, D. *Phys. Rev. E* **1994**, *50*, 4780.

(25) Iannacchione, G. S.; Mang, J. T.; Kumar, S.; Finotello, D. *Phys. Rev. Lett.* **1994**, *73*, 2708.

(26) Rozanski, S. A.; Stannarius, R.; Groothues, H.; Kremer, F. *Liq. Cryst.* **1996**, *20*, 59.

(27) Aliev, F. M.; Sinha, G. P. *Mol.Crys.Liq.Crys.* **1997**, *303*, 325.

(28) Zalar, B.; Zumer, S.; Finotello, D. *Phys. Rev. Lett.* **2000**, *84*, 4866.

(29) Aliev, F. M.; Nazario, Z.; Sinha, G. P. *J. Non-Cryst. Solids* **2002**, *305*, 218.

(30) Liu, X.; Allender, D. W.; Finotello, D. *Europhys. Lett.* **2002**, *59*, 848.

(31) Zalar, B.; Blinc, R.; Zumer, S.; Jin, T.; Finotello, D. *Phys. Rev. E* **2002**, *65*, 041703.

(32) Leys, J.; Sinha, G.; Glorieux, C.; Thoen, J. *Phys. Rev. E* **2005**, *71*, 051709.

(33) Jin, T.; Zalar, B.; Lebar, A.; Vilfan, M.; Zumer, S.; Finotello, D. *Eur. Phys. J. E* **2005**, *16*, 159.

(34) Sinha, G.; Leys, J.; Glorieux, C.; Thoen, J. *Phys. Rev. E* **2005**, *72*, 051710.

(35) Rozanski, S. A.; Thoen, J. *Liq. Cryst.* **2006**, *33*, 1043.

(36) Diez, S.; Pérez-Jubindo, M. A.; de la Fuente, M. R.; López, D. O.; Salud, J.; Tamarit, J. Ll. *Liq.Cryst.* **2006**, *33*, 1083.

(37) Diez, S.; López, D. O.; de la Fuente, M. R.; Pérez-Jubindo, M. A.; Salud, J.; Tamarit, J. Ll. *J. Phys. Chem. B* **2005**, *109*, 23209.

(38) Diez, S.; Pérez-Jubindo, M. A.; de la Fuente, M. R.; López, D. O.; Salud, J.; Tamarit, J. Ll. *Chem. Phys. Lett.* **2006**, *423*, 463.

(39) Pérez-Jubindo, M. A.; de la Fuente, M. R.; Diez-Berart, S.; López, D. O.; Salud, J. *J. Phys. Chem. B* **2008**, *112*, 6567.

(40) Emsley, J. W.; Luckhurst, G. R.; Shilstone, G. N.; Sage, I. C. *Mol. Cryst. Liq. Cryst. Lett.* **1984**, *102*, 223.

(41) Attard, G. S.; Date, R. W.; Imrie, C. T.; Luckhurst, G. R.; Roskilly, S. J.; Seddon, J. M.; Taylor, L. *Liq. Cryst.* **1994**, *16*, 529.

(42) Sied, M. B.; Salud, J.; López, D. O.; Barrio, M.; Tamarit, J. Ll. *Phys. Chem. Chem. Phys. (PCCP)* **2002**, *4*, 2587.

(43) Nordio, P. L.; Rigatti, G.; Segre, U. *Mol. Phys.* **1973**, *25*, 129.

(44) Crawford, G. P.; Allender, D. W.; Doane, J. W. *Phys. Rev. A* **1992**, *45*, 8693.

(45) Guyot-Sionnest, P.; Hsiung, H.; Shen, Y. R. *Phys. Rev. Lett.* **1986**, *57*, 2963.

(46) Brás, A. R.; Dionísio, M.; Schönals, A. *J. Phys. Chem. B* **2008**, *112*, 8227.

(47) Cusmin, P.; de la Fuente, M. R.; Salud, J.; Pérez-Jubindo, M. A.; Diez-Berart, S.; López, D. O. *J. Phys. Chem. B* **2007**, *111*, 8974.

JP9121084